1 **Projected increases in wildfires may challenge regulatory curtailment of PM[2.5] over the**

2 **eastern US by 2050**

4 Chandan Sarangi[1,2]*, Yun Qian[2]*, L. Ruby Leung[2], Yang Zhang[3], Yufei Zou[4,2], Yuhang

5 Wang[4]

7 [1] Indian Institute of Technology Madras, Chennai, India

8 [2] Pacific Northwest National Laboratory, Richland, WA, USA

9 [3] Department of Civil and Environmental Engineering, Northeastern University, Boston, MA

10 [4] School of Earth and Atmospheric Sciences, Georgia Institute of Technology, Atlanta, GA,

11 USA.

14 *Corresponding Authors:

15 chandansarangi@iitm.ac.in

16 yun.qian@pnnl.gov

21 **Abstract**

22 Anthropogenic contribution to the overall fine particulate matter ($PM_{2.5}$) concentrations has

23 been declining sharply in North America. In contrast, a steep rise in wildfire-induced air

24 pollution events with recent warming is evident in the region. Here, based on coupled fire-

25 climate-ecosystem model simulations, summertime wildfire-induced $PM_{2.5}$ concentrations are

26 projected to nearly double in North America by the mid-21st century compared to the

27 present. More strikingly, the projected enhancement in fire-induced $PM_{2.5}$ (~ 1-2 $\mu g/m^3$) and

28 its contribution (~15-20%) to the total $PM_{2.5}$ are distinctively significant in the eastern US.

29 This can be attributed to downwind transport of smoke from future enhancement of wildfires

30 in North America to the eastern US and associated positive climatic feedback on $PM_{2.5}$ i.e.

31 increased atmospheric stability and reduced precipitation. Therefore, the anticipated

32 reductions in $PM_{2.5}$ from regulatory controls on anthropogenic emissions could be

33 significantly compromised in the future in the densely populated eastern US.

34 **Key points:**

35   1) Wildfire-$PM_{2.5}$ associations studied based on unprecedented two-way coupled fire-

36   climate-ecosystem model simulations

37   2) A steep rise in wildfire-induced air pollution events with recent warming is evident in

38   the region

39   3) The transported smoke from enhanced wildfires in North America can severely affect

40   air quality over Eastern US

41

42 **Keywords:** wildfire emissions, climate change, air quality, smoke transport, wildfire-climate-

43 ecosystem interactions

1. __Introduction__

Wildfires are widespread burning events in forests, shrub lands, and grazing lands. In North America (mainly Canada and the US), particulate matter emissions from wildfires are a significant source of regional air pollution (Shi et al., 2019; McClure and Jaffe, 2018; Van Der Werf et al., 2010; Jaffe et al., 2008). Since the 1980s, the number of large wildfires and the length of wildfire season have been increasing, and the trends are projected to continue in the future over the western US, Alaska and Canada (Kitzberger et al., 2017; Kirchmeier-Young et al., 2017; Abatzoglou and Williams, 2016; Partain et al., 2016; Jolly et al., 2015; Westerling et al., 2006; Gillett et al., 2004). Accordingly, particulate emissions from wildfires are also anticipated to increase in North America in the 21st century (Knorr et al., 2017; Liu et al., 2016; Val Martin et al., 2015). Human exposure to high concentrations of wildfire-emitted airborne particulate matter of diameter ≤2.5 μm ($PM_{2.5}$) is known to have substantial adverse effects on pulmonary and cardiovascular functioning (Anjali et al., 2019; Black et al., 2017), which contribute significantly to global and regional all-cause mortality (Zhang et al., 2020; Hong et al., 2019; Yang et al., 2019; Ford et al., 2018; Johnston. et al., 2012). Therefore, a better understanding of the future changes in wildfire-induced $PM_{2.5}$ and its contribution to the total surface $PM_{2.5}$ is essential.

In the last two decades, ambient air quality in the US has substantially improved due to a decline in $PM_{2.5}$ by ~ 40 % (US EPA, 2018). The decrease in $PM_{2.5}$ is primarily due to curtailment of anthropogenic emissions resulting from US-based efforts to meet regulations such as the Clean Air Act (US EPA, 2009), Cross-State Air Pollution Rule, Regional Haze Rule, and the motor vehicles emissions standards. Consequently, air quality over the contiguous US (CONUS) and Canada has improved steadily such that it is predicted to achieve the targeted National Ambient Air Quality Standards in the future (Nolte et al.,

68   2018). Under this promising scenario, the influence of wildfire-emissions on the total $PM_{2.5}$

69   becomes even more crucial. Depending on the competition between climate-induced increase

70   in wildfires and the regulatory control on anthropogenic emissions, future enhancement in

71   wildfire-induced $PM_{2.5}$ may compromise the reduction in anthropogenic $PM_{2.5}$ concentrations

72   in certain regions. In agreement, recent studies have highlighted the potential for future

73   enhancement in wildfire-induced pollution to diminish the reducing trend in $PM_{2.5}$, primarily

74   over the western US (O'Dell et al., 2019; Ford et al., 2018; Val Martin et al., 2015; Yue et al.,

75   2013).

76   While the fractional wildfire burnt area and fire intensities are the greatest over the

77   western US and Canadian regions within North America, anthropogenic emissions dominate

78   the ambient $PM_{2.5}$ concentration over the eastern US. The inherent geographical separation

79   between the regions with large wildfire emissions and anthropogenic emissions leads to a

80   pertinent question: will future enhancement in wildfires over the western US and Canada

81   have significant effects on $PM_{2.5}$ over the eastern US? Addressing this question is crucial

82   because the declining trend in $PM_{2.5}$ over the eastern US is the major contributor to the

83   observed 40% decrease in $PM_{2.5}$ over the US in the last two decades (US EPA, 2018).

84   Eastward advection of wildfire smoke from Canada and the western US has been found to

85   severely hamper the surface air quality of the central and eastern US under the influence of

86   the prevailing westerlies during the summer months (Brey et al., 2018; Wu et al., 2018;

87   Gunsch et al., 2018; Kaulfus et al., 2017; Dempsey, 2013). The transported wildfire smoke

88   can influence the meteorology and climate via the radiative impact of carbonaceous

89   emissions, changes in land albedo and cloud system perturbations (Ward et al., 2012; Liu et

90   al., 2014). These fire-weather interactions can have positive feedback on the locally-emitted

91    $PM_{2.5}$ in the eastern US by surface cooling and boundary layer suppression(Guan et al.,

92   2020). At the same time, fire-triggered ecosystem changes can induce negative feedback on

93 PM2.5 by reducing the future wildfires over North America (Zou et al., 2020). Thus, two-

94 way interactions between fires and climate that are important for predicting future changes in

95 wildfire locations, intensities, and durations (Harris et al., 2016) as well as associated

96 particulate emissions is essential. However, past studies have mostly employed simple

97 statistical models based on statistical regressions of present-day fire burnt area on the

98 meteorological fields (Liu et al., 2016; Spracklen et al., 2009; Yue et al., 2013; Val Martin et

99 al., 2015), and more recently, one-way coupled modelling (Ford et al., 2018; O'Dell et al.,

100 2019).

101   Here, based on new two-way coupled fire-climate-ecosystem simulations, we

102 demonstrate the significance of wildfire-induced contributions to ambient $PM_{2.5}$ over the

103 eastern US due to enhanced wildfire smoke transportation and smoke-induced changes in

104 weather in eastern US. This enhancement in wildfire-induced $PM_{2.5}$ may potentially challenge

105 the targeted policy-driven reduction of $PM_{2.5}$ in the eastern US. Next, our model setup,

106 experiments and methodology are explained in Section 2, followed by results and discussion

107 in Section 3. The study is summarized in Section 4.

108   **2.   Materials and Methods**

109   **2.1. RESFire-CESM Model description**

110   We employ the open-source REgion-Specific ecosystem feedback fire (RESFire)

111 model coupled with the Community Land Model version 4.5 and the Community

112 Atmosphere Model version 5 (CAM5) of the Community Earth System Model (CESM)

113 version 1 (Zou et al., 2019; Neale et al., 2013) to perform two-way coupled simulations.

114 RESFire provides state-of-the-art capabilities to simulate the complex fire-climate-ecosystem

115 interactions globally for fires occurring over wildland, cropland, and peatland. Although

116 wildfires dominate in the North American region, RESFire simulates both wildfires and

117 prescribed fires. Moreover, this integrated setup includes climatic feedback from fire-induced

118 aerosol direct and indirect radiative effects and associated weather changes. It also includes

119 feedback from fire-induced vegetation distribution changes and associated biophysical

120 processes such as evapotranspiration and surface albedo. Sofiev et al. (2012) described the

121 fire plume rise parameterization. Other features in CLM4.5 and CAM5, such as the

122 photosynthesis scheme (Sun et al., 2012), the MAM3 aerosol module (Liu et al., 2012), and

123 the cloud macrophysics scheme (Park et al., 2014), allow for more comprehensive

124 assessments of the climate effects of fires through their interactions with vegetation and

125 clouds. Fire-ecosystem interactions are modelled by simulating fire-induced vegetation

126 mortality and regrowth (and associated land cover change) in RESFire. This approach has

127 been introduced in Zou et al. (2019) and the simulated ecological and climatic effects of

128 wildfires have been evaluated in two sets of sensitivity experiments in Zou et al. (2020).

129 Although fire-climate-ecosystem interactions are considered in this study, our focus is on the

130 fire-induced changes in $PM_{2.5}$ over Canada and the US, so the two vegetation-focused

131 sensitivity experiments reported in Zou et al. (2020) are not included in this paper. Please

132 refer to Zou et al. (2019) and Zou et al. (2020) for more details about the simulation of fire-

133 ecosystem interactions.

134 **2.2 Numerical Experiment and Methodology**

135 We designed two sets of simulations for the present day and future scenarios to

136 quantify the impacts of fire-climate-ecosystem interactions (Table 1). The spatial resolution is

137 0.9° (lat) × 1.25° (lon) with a time step of 30 min. In each set of simulations, we conducted a

138 default all emission included control run (X_{ALL}, where x=2000 or 2050 indicates the present

139 day or future, respectively) and a sensitivity run with no wildfire emissions to the atmosphere

140 (X_{WEF}, where X is the same as for the control runs). The ALL runs are designed to simulate

141 fully interactive fire disturbances such as fire emissions with plume rise and fire induced land

142   cover changes of the present day (representative of the 2000s, 2000ALL) and a moderate future

143   emission scenario (representative of the 2050s, 2050ALL) via the RCP4.5. The only difference

144   between the ALL and WEF scenario is that wildfire emissions are absent in the WEF

145   scenario. Specifically, in the WEF runs, the online simulated fire emissions are not passed to

146   the CAM5 atmosphere model so that the difference between the ALL and WEF runs can be

147   used to isolate the atmospheric impacts of fire-climate interactions.

148   Table 1: Summary of the sensitivity simulations performed

Scenario	Present-day		Future	
Experiment Name	2000ALL	2000WEF	2050ALL	2050WEF
Simulation years	2001-2010	2001-2010	2051-2060	2051-2060
Atmosphere	CAM5	CAM5	CAM5	CAM5
Land	CLM4.5	CLM4.5	CLM4.5	CLM4.5
Ocean	Climatology	Climatology	RCP4.5	RCP4.5
Sea ice	Climatology	Climatology	RCP4.5	RCP4.5
Non-fire emissions	ACCMIP	ACCMIP	RCP4.5	RCP4.5
Fire emissions	Online fire aerosols with plume rise	—	Online fire aerosols with plume rise	—
Land cover	Fire disturbances on present-day condition	Fire disturbances on present-day condition	Fire disturbances on RCP4.5 condition	Fire disturbances on RCP4.5 condition

149

150   For the present-day experiments, we used the spun-up states from Zou et al. (2019) as

151   initial conditions for both meteorological and chemical variables. Sea surface temperature

152   (SST) for the present day was obtained from the Met Office Hadley Centre (HadISST).

153   Present-day non-fire emissions from anthropogenic and other sources were based on

154   ACCMIP (Lamarque et al., 2010) for the year 2000. We replaced the prescribed GFED2 fire

155   emissions (van der Werf et al., 2006) in the default setting of CESM with the online-coupled

156   fire emissions generated by the RESFire model. Zou et al. (2019) provided more details of

157   the physics parameterizations and modeling experiment settings used in these simulations.

158 Land use and land cover data for 2000 and 2050 from the Land-Use History A product (Hurtt

159 et al., 2006) are used to initialize the $2000_{ALL}/2000_{WEF}$ and $2050_{ALL}/2050_{WEF}$ simulations,

160 respectively. Following the above setup, the future scenario 2050_{ALL} experiment accounts for

161 both fuel load changes associated with the projected land use and land cover change

162 (LULCC) in the 2050s and fire weather changes driven by the SST and sea ice forcing from a

163 coupled CESM simulation following the greenhouse gas (GHG) forcing of the RCP4.5

164 scenario. The global mean GHG mixing ratios in the CAM5 atmosphere model were fixed at

165 the year 2000 levels in all the present-day experiments and they were replaced by those of the

166 RCP4.5 scenario with the well-mixed assumption and monthly variations. However, the

167 future population and socioeconomic conditions were identical to those of the present day so

168 there was no explicit impact of human-induced mitigation/enhancement effects on wildfires

169 in the future projection in all the future experiments. Future human impacts were considered

170 implicitly in LULCC-induced fuel load changes in the RCP4.5 scenario.

171   The net projected changes by 2050s in emissions, meteorology and air quality during

172 summer (JJA) months are estimated by comparing decadal-mean values simulated by

173 2000_{ALL} with 2050_{ALL}. Wildfire-induced enhancement in $PM_{2.5}$ concentration in the present

174 day and mid-21st century is estimated by comparing 2000_{ALL} with 2000_{WEF} and 2050_{ALL} with

175 2050_{WEF}, respectively. Further, the projected increase in wildfire-induced $PM_{2.5}$ in the future

176 is calculated by comparing the simulated wildfire effect of the 2050s ($2050_{ALL}-2050_{WEF}$) with

177 that of the 2000s ($2000_{ALL}-2000_{WEF}$). With large spatiotemporal variability, the projected

178 changes in transported fire-emissions from the western US and Canada to the eastern US by

179 the 2050s and the corresponding impacts are summarized using probability distribution

180 functions. The latter provide information not only for the mean but also variability and

181 extreme values to quantify the simulated changes for the three subregions.

182

3. Results and Discussion

183

3.1 Model Evaluation

184

185   Zou et al. (2019) performed comprehensive evaluation of the RESFire simulated

186   wildfire burnt area distribution, associated carbon emissions and terrestrial carbon balance to

187   demonstrate reasonable model skill. Zou et al. (2020) compares global fire simulations by

188   CESM-RESFire with modeling results reported in the literature to show better agreement

189   with the GFED4.1s benchmark data and predicts more prominent changes in the future than

190   those predicted by Kloster et al. (2010, 2012). These differences might come from differences

191   in the climate sensitivities of the fire models and scenarios and other input data used to make

192   future projections.

193   Here, we evaluate the simulated surface $PM_{2.5}$ against satellite-estimates (Figures 1)

194   over North America. The $PM_{2.5}$ concentration is calculated as the sum of sulfate, nitrate, fine

195   sea salt (first 2 size bins), fine dust (first size bin), black carbon (BC), and organic aerosol

196   (OC) at the surface-level of model. OC is the sum of primary organic matter (POM) and

197   secondary organic aerosol (SOA), and SOA is the sum of secondary species formed from

198   toluene, monoterpenes, isoprene, benzene, and xylene. Figure 1 compares the observed and

199   simulated mean annual $PM_{2.5}$ averaged over 2001-2010. The 10-year average satellite AOD-

200   derived annual mean surface $PM_{2.5}$ concentrations (Van Donkelaar et al., 2018) are regridded

201   to the model grid (Figure 1A) and then compared with the RESFire simulations in the

202   2000$_{ALL}$ present-day run (Figure 1B). The spatial distribution of annual surface $PM_{2.5}$ is

203   reasonably well simulated but also have some biases. To quantify the biases, we also

204   estimated the correlation coefficient as well as normalized mean biases (NMB) of the

205   simulated values compared against the satellite retrieved values over two subregions.

206   Quantitatively, the NMB values over the western US (WUS) and eastern US (EUS) are 18%

207   and 7%, respectively (Figure 1C-D). In addition, the spatial variability of the 2001-2010

208   averaged annual AOD distribution (Supplementary Figure 1) is also well represented in our

209   simulation, although the model underestimates high AOD values. Similar spatial variability

210   and biases in AOD and $PM_{2.5}$ were also found when a comparison was performed for only

211   summer months (JJA). Our simulation biases are within the uncertainty range among the

212   various satellite and ground-based datasets, which have normalized mean biases ranging from

213   -3.3% to 33.3% when benchmarked against the ground-based IMPROVE data over the

214   contiguous US (Diao et al., 2019). Val Martin et al. (2015) also reported a similar range of

215   biases of $PM_{2.5}$ in their simulation over the US.

216   Discrepancies between the simulated and observed $PM_{2.5}$ values may be attributed to

217   several potential reasons. First, the satellite-derived data has a non-zero lower bound of $PM_{2.5}$

218   concentrations, so the ambient background concentrations for pristine regions such as the

219   remote areas in Alaska, Canada, and the western US may be overestimated. Second, year

220   2000-based constant non-fire emissions were used in the RESFire simulation, which may

221   result in overestimation of the $PM_{2.5}$ concentrations from non-fire sources during 2001-2010

222   when anthropogenic emissions and $PM_{2.5}$ concentrations continue to decrease (US EPA,

223   2018). This overestimation is prominent in regions dominated by non-fire sources such as the

224   southeastern US. Third, large uncertainties in fuel consumption and emission factors preclude

225   an accurate estimation of the primary fire emissions in the model, especially for the eastern

226   US where large fractions of low-intensity prescribed fires consume only under-canopy fuels

227   such as litter and duff layers. The fire model may fail to capture the subtle distinctions

228   between low-intensity prescribed fires and forest fires, so more fuels are consumed and result

229   in higher emissions. Lastly, comparison of a coarsely resolved simulation against in-situ

230   observations also contributes to uncertainty. Differences in the degree to which fire-climate

231   interactions and other physical processes and feedbacks are represented by the models can

232   explain the slights differences in estimating the present day mean wildfire-induced change in

233   PM$_{2.5}$ over local and downwind regions between our simulations and previous studies.

234   Nonetheless, reasonable simulation of the spatial distribution of wildfire burnt area, AOD,

235   and near surface particulate concentration (mean bias of ~10-20 %) instills confidence about

236   the fidelity of our model setup in particulate pollution simulation, which is the focus of this

237   study.
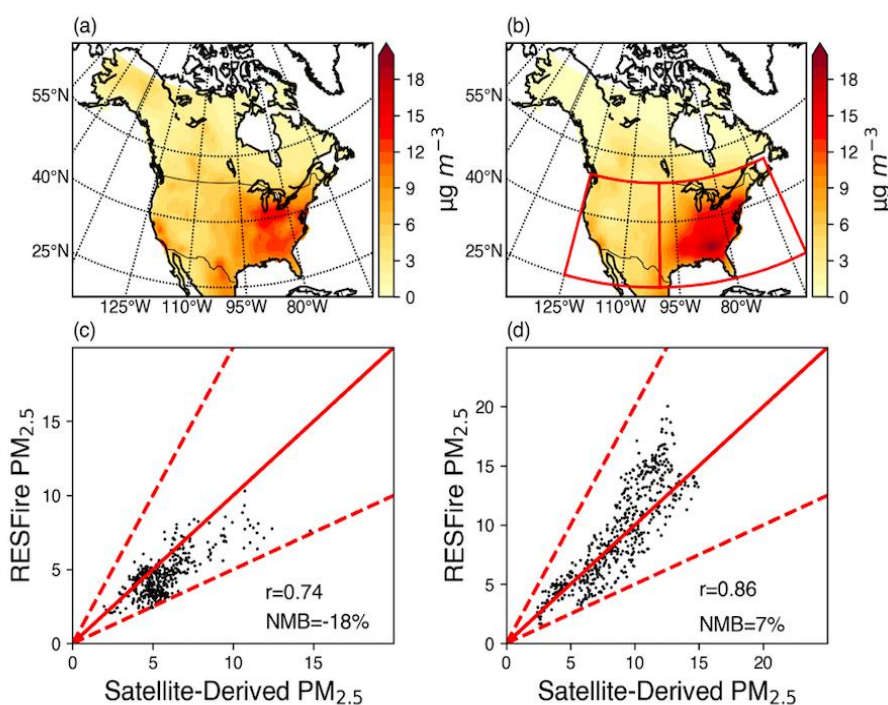
238

239

240   Figure 1: Comparison of the 10-year (2001-2010) averaged annual mean surface PM$_{2.5}$
241   concentration between observations and RESFire simulations. (a) Satellite-derived surface
242   PM$_{2.5}$ concentrations (with dust and sea-salt removed) estimated by Donkelaar et al., 2018
243   (available at https://sedac.ciesin.columbia.edu/data/set/sdei-global-annual-gwr-pm2-5-modis-
244   misr-seawifs-aod; last access: 5 November, 2021); (b) 2000$_{ALL}$ Simulated surface PM$_{2.5}$
245   concentrations (with dust and sea-salt removed) averaged over 2001-2010; The red boxes
246   denote the two subregions (EUS and WUS) shown in Fig. 2 in the main text. (c) comparison
247   of simulated and satellite based gridded surface PM$_{2.5}$ concentrations in the WUS subregion;
248   (d) same as (c) but in the EUS subregion. The red solid and dashed lines denote the 1:1 ratio
249   line and ±100% biases, respectively. The correlation coefficients and NMB values are shown
250   at the lower-right corner of each subplot.

251

3.2 Fire-induced changes in burnt area and $PM_{2.5}$

252

253 The decadal-mean annual fire burnt area simulated for the present day shows

254 widespread wildfires over the entire North America (Figure 2A). Specifically, Canada and the

255 forested areas of the northwestern (> 36 N latitude) and southeastern (< 36 N latitude) US are

256 most intensely affected by wildfires in the present day. By the mid-21st century, a striking

257 increase of 2-5 times in fire burnt area is projected over Canada, Alaska, the Pacific

258 Northwest and portions of the western US by the 2050s (Figure 2B). A distinct positive shift

259 in the probability density function (PDF) of annual fire burnt area is evident in the future,

260 with the decadal-mean difference statistically significant at the 99% confidence level (Zou et

261 al., 2020). A small and statistically insignificant change in interannual variability (~ 0.4 Mha

262 yr^{-1}) of fire burnt areas is also simulated between the present and future. Specifically, our

263 model predicts more than a doubling of burnt area in boreal regions of Canada in the future,

264 in line with a previous projection for Canada (Wotton et al., 2017). Future enhancement in

265 fire burnt area is ~ 20-50% in most fire grids over the western coast of US, which is higher

266 than that over the eastern US (Figures 2A and 2C). The increase over the western US is closer

267 to the lower bound of that derived from statistical model ensemble projections for the western

268 US in the mid-21st century (Yue et al., 2013). The statistics-based projections of future burnt

269 area over North America were likely too high because fire-induced land cover change, fuel

270 load reduction and factors could induce a negative fire feedback, which was not considered in

271 previous fire projection studies (Zou et al. 2020).

272 Annual fire burnt area in the southeastern US shows a decline in the future (Figure

273 2C), as precipitation is projected to increase in that region (discussed later). Note that all

274 future fire changes between 2050_{ALL} and 2000_{ALL} are primarily associated with climate

275 warming in response to the increase in greenhouse gas (GHG) concentrations in the RCP4.5

276 scenario. No direct impacts of population and socioeconomic changes on wildfires are

277   included in our simulations, although these factors contribute to changes in GHG emissions

278   (via the RCP scenario) that influence the climate simulated in 2000_{ALL} and 2050_{ALL}. As about

279   80% of the projected fire changes in the future is restricted to the summer season (June

280   through August; JJA) (Figure 2D), we focus on analysis of the summer-mean wildfire-

281   induced $PM_{2.5}$ and its projected future changes over North America.
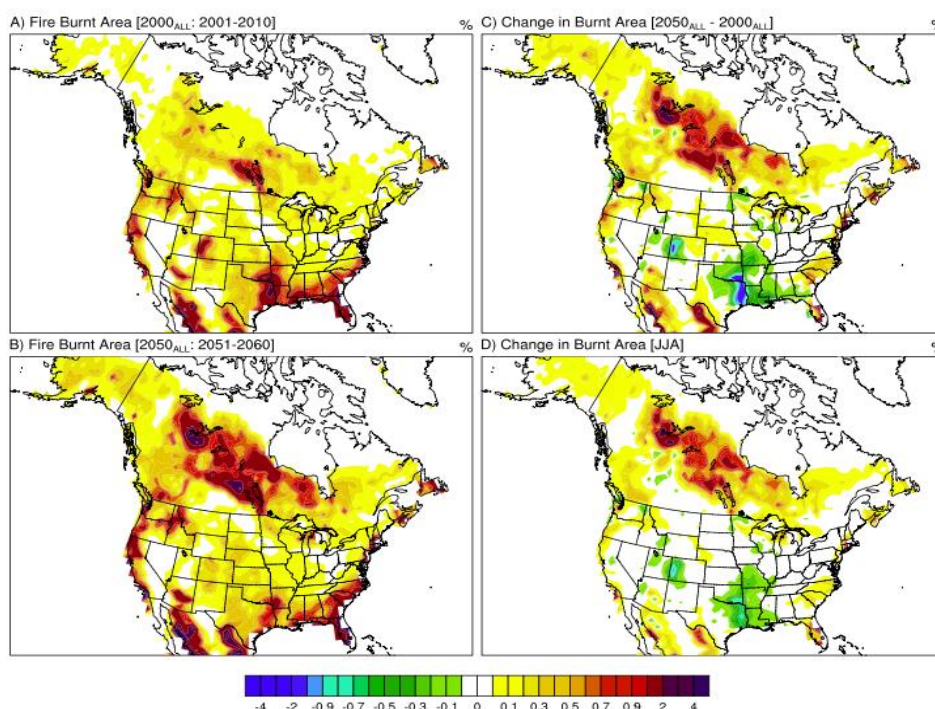
282

283   Figure 2: **Spatial distribution of fire burnt area. A-D**, Spatial distribution of simulated
284   decadal-mean annual burnt area (as percentage) over North America for present day (A),
285   mid-21st century (B) and the net change between the 2050s and the 2000s (C). **D**, same as
286   (C), but for wildfire burnt area during summer only (June through August; JJA). The colorbar
287   illustrate grid fraction of area burnt.

288
289   The simulated 10-year averaged summer-mean wildfire-induced $PM_{2.5}$ values in

290   2000_{ALL} are more than 0.5 µg/m^3 over a large part of North America in the present day, with

291   noticeably larger values (> 1 µg/m^3) in Canada and the northwestern, central, and

292   southeastern US (Figure 3A). Interestingly, the spatial distribution of wildfire-induced

293    $PM_{2.5} > 1 \ \mu g/m^3$ resembles an inverted horse-shoe shape. The inverted horse-shoe shaped

294   spatial distribution is also consistent with the wildfire-smoke climatology derived from the

295   satellite-guided operational smoke product of the Hazard Mapping System (HMS) during

296   2005-2015 (Brey et al., 2018; Kaulfus et al., 2017). By the mid-21st century, the spatial extent

297   of the horse-shoe shape for areas with wildfire-induced $PM_{2.5}$ enhancement $> 1 \ \mu g/m^3$

298   expands significantly to span most regions of North America, with the most pronounced

299   enhancement occurring over Canada (Figure 3B). The PDFs of the spatial distribution for the

300   three regions can be seen in Figure 3C-E. Specifically, wildfire induced $PM_{2.5}$ in the 2000s

301   over Canada, WUS and EUS during summer is ~ 1-3 $\mu g/m^3$, 1-3 $\mu g/m^3$ and 0.6-1.2 $\mu g/m^3$,

302   respectively. Maximum values within the WUS region are found over the Pacific Northwest,

303   with most areas having wildfire induced $PM_{2.5}$ values of ~ 2-3 $\mu g/m^3$. Similarly, the southern

304   states have relatively high wildfire induced $PM_{2.5}$ concentrations of ~ 2-4 $\mu g/m^3$ within the

305   EUS in the present-day simulation.

306   Compared to the 2000s, the wildfire induced JJA averaged $PM_{2.5}$ values are almost

307   doubled to ~ 3-6 $\mu g/m^3$ over Canada in the 2050s (Figure 3B and Figure 3C). Consistently,

308   the values of wildfire induced PM2.5 over WUS (mainly coastal) also doubled in 2050s

309   compared to 2000s, with modal values of ~ 2-2.5 $\mu g/m^3$ (Figure 3D). Most interestingly, the

310   enhancement in wildfire-induced summer-mean $PM_{2.5}$ over the northern EUS is also

311   significant by the 2050s (Figures 3B). Largely, the summer-mean wildfire-induced $PM_{2.5}$

312   concentration over EUS increases from ~0.8 to ~2 $\mu g/m^3$ in the mid-century to values of 1.2-

313   3.0 $\mu g/m^3$ (Figure 3E). The summer-mean wildfire-induced $PM_{2.5}$ is thus projected to double

314   in North America by the 2050s compared to the 2000s, with a substantial coverage over the

315   EUS. Also, the spatial variability is enhanced which will enhance the exposure over

316   previously clean grids. An important finding from these PDFs appears to be that there are

317   fewer grids with < 1 $\mu g/m^3$ wildfire induced PM2.5, or alternatively, that more regions are

318   being influenced by PM$_{2.5}$, and many areas that were already seeing wildfire impacts are

319   seeing enhanced impacts. Such enhancement is found not only at the surface but also in an

320   elevated atmospheric layer over EUS between 900 and 700 hPa. This is nonintuitive given

321   the fact that the increase in fire-burnt area by mid-century over the EUS is not substantial.
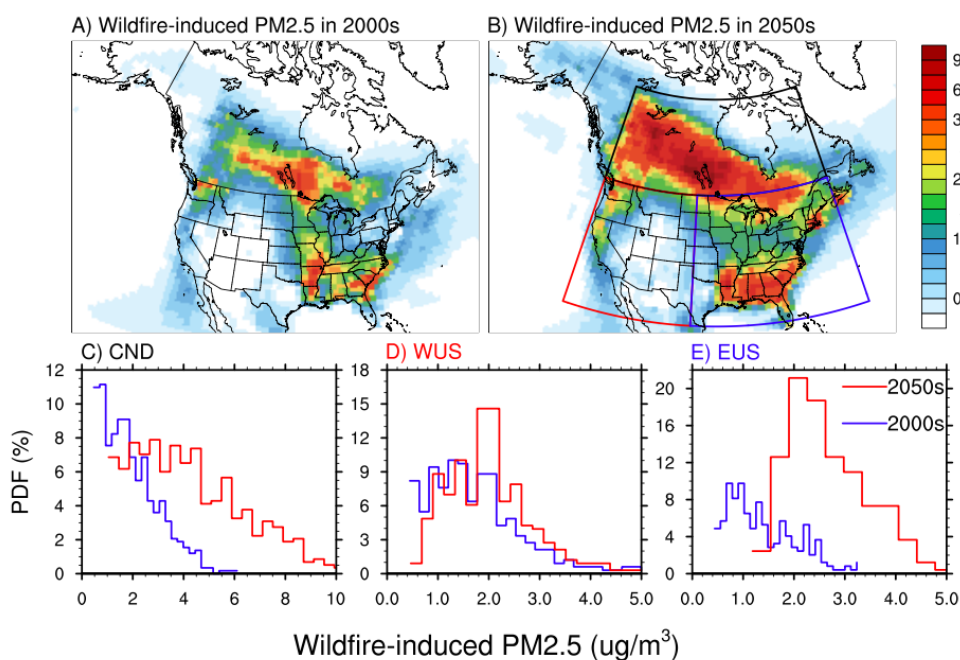
322

323   Figure 3: **Spatial distribution of** PM$_{2.5}$ **concentrations.** Spatial distribution of decadal-mean
324   wildfire-induced enhancement in summer (JJA) PM$_{2.5}$ concentration over North America for
325   present day (A, 2000$_{ALL}$-2000$_{WEF}$) and future (B, 2050$_{ALL}$-2050$_{WEF}$). **C-E**, Probability density
326   functions (PDFs) of wildfire contribution within the three regions shown in Figure 2B for
327   Canada (CND: black box) (C), WUS (red box) (D), and EUS (blue box) (E), respectively, for
328   2000s (blue) and 2050s (red). Only grids over land in North America are used to generate
329   the PDFs. The y-axis indicates the probability of occurrence of different PM$_{2.5}$ values shown
330   in the x-axis. The colorbar illustrates PM2.5 in ug/m^3.
331

332   As anthropogenic- and wildfire-induced PM$_{2.5}$ concentrations may change differently

333   with time across North America, next, we investigate the relative contribution of wildfire-

334   induced PM$_{2.5}$ to the total PM$_{2.5}$ in the future. Prominent enhancement of the wildfire

335   contribution is apparent in the entire domain by the 2050s (Figures 4A-B). Largely, during

336   the 2000s, the simulated fractional contribution of wildfires to $PM_{2.5}$ is ~15-50 % in Canada

337   (Figure 4A). Specifically, a bi-modal distribution is simulated over Canada with modal values

338   around 18% and 30% (Figure 4C). Over WUS, the present day simulated percentage

339   contributions of wildfire-induced values are 5-25% (Figure 4A), with modal values between

340   10-20% (Figure 4D). Note that many areas located in the Pacific Northwest have higher

341   values of ~30-40% (Figure 4A). At the same time, the fractional contribution by wildfire-

342   induced $PM_{2.5}$ is ~5-10% in most areas of EUS in present day (Figure 4F). Nevertheless,

343   some areas in the central US also have higher values of ~10-25% (Figure 4A).
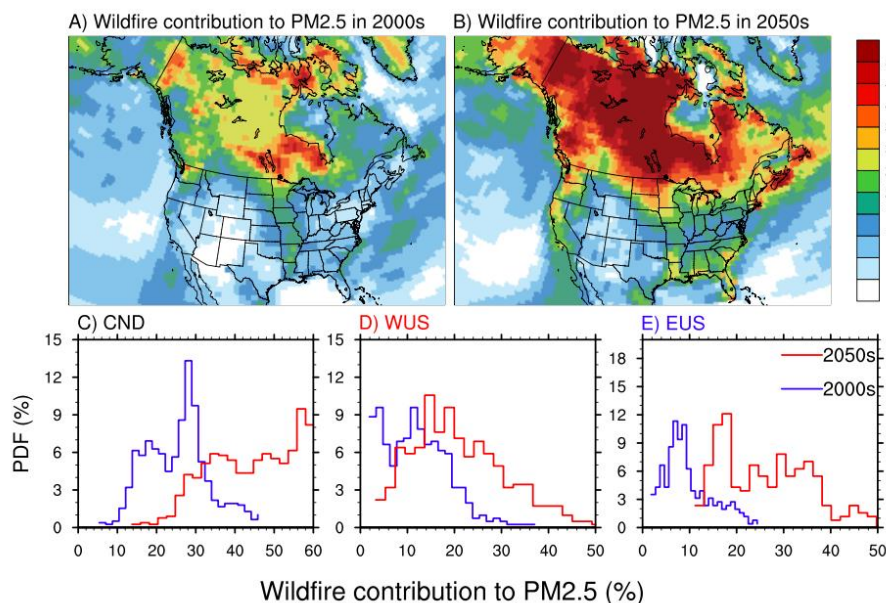
344

345   Figure 4: **Spatial distribution and probability density function of the percentage**

346   **contribution of wildfire emissions. A-B**, Spatial distribution of the percentage contribution

347   of wildfire emissions to decadal-averaged summer (JJA) mean $PM_{2.5}$ concentrations over

348   North America during present day (A) and future (B). The percentage contribution of

349   wildfire-induced $PM_{2.5}$ to the total $PM_{2.5}$ concentrations is calculated as ([2000$_{ALL}$-

350   2000$_{WEF}$]/2000$_{ALL}$) and ([2050$_{ALL}$-2050$_{WEF}$]/2050$_{ALL}$) for the present and future, respectively.

351   **C-E**, Probability density functions (PDFs) of the percentage wildfire contribution within the

352 three regions shown in Figure 2D for Canada (CND: black box) (C), WUS (red box) (D), and

353 EUS (blue box) (E), respectively, for the 2000s (blue) and the 2050s (red). Only grids over

354 land in North America are used to generate the PDFs. The y-axis indicates the probability of

355 occurrence of different $PM_{2.5}$ values shown in the x-axis.

356

357   The wildfire contributions in the 2050s show a clear shift towards higher values in all

358 sub-regions compared to the 2000s (Figure 4B). Over Canada, the values shifted from 15-30

359 % in the 2000s to ~30-60% in the 2050s, a nearly two-fold increase in the fractional

360 contribution of wildfire emissions to the total $PM_{2.5}$ concentration is simulated (Figure 4B

361 and corresponding PDF in Figure 4C). Similarly, the contribution values increased to ~ 10-35

362 % in the 2050s, compared to 10-20% in the 2000s over WUS (Figure 4B), thereby featuring a

363 broadening of the bi-modal distribution of wildfire contribution (Figure 4D). The shift in the

364 percentage contribution is most prominent for the higher values, corresponding to some areas

365 located in the Pacific Northwest and west coast of the US (Figure 4B). Consistent with Figure

366 3B, the shift in the contribution values over EUS is also very distinct, revealing an increase in

367 the mode values from 6-10% in the 2000s to ~16-20 % by the 2050s (Figure 4B and Figure

368 4E). Thus, not only in absolute values, but our results also underscore a large increase in the

369 contribution of wildfire emissions over EUS in the future.

370 **3.3. Mechanistic understanding of the underlying processes**

371   The larger enhancement in the relative contribution of wildfire emissions to the total

372 surface $PM_{2.5}$ in EUS in the 2050s can be explained by three mechanisms. First, due to the

373 increase in Canadian and western US wildfires, downwind transport of wildfire smoke

374 plumes to EUS will be enhanced by the 2050s. This long-range transport to the atmospheric

375 column of EUS can happen within a few days of the fire occurrence (Supplementary Figures

376 2A and 2B). Using Hazard Mapping System (HMS)-detected smoke plumes, recent studies

377 identified a strong positive association between the transported smoke plumes in the

378   atmospheric column and collocated surface PM2.5 enhancement in EUS (Brey et al., 2018;

379   Wu et al., 2018; Gunsch et al., 2018; Kaulfus et al., 2017; Larsen et al., 2017; Dempsey,

380   2013). Hazard Mapping System (HMS) is an operational smoke detection product over North

381   America known as developed by the National Oceanic and Atmospheric Administration

382   (NOAA) and operated by National Environmental Satellite, Data, and Information Service

383   (NESDIS), available at http://satepsanone.nesdis.noaa.gov/FIRE/fire.html. Specifically, these

384   studies found that the smoke plumes transported from Canada are located at an altitude of ~

385   1-3 km over EUS (Colarco et al., 2004; Wu et al., 2018). Due to mixing by the daytime

386   boundary layer and deposition, the smoke plumes enhance the surface $PM_{2.5}$ concentration

387   over EUS (Wu et al., 2018; Colarco et al., 2004; Rogers et al., 2020; Dreessen et al., 2015).

388   Hence HMS smoky days may be a useful proxy for wildfire-induced surface PM2.5 over

389   North America. In agreement, Brey et al. (2018) showed that the HMS-based smoke plumes

390   observed over EUS is significantly aged, suggestive of their long-range transport origin.

391   Consistent with the observed temporal change in HMS pattern, Xue et al. (2021) estimated

392   using the mid-visible Multi Angle Implementation of Atmospheric Correction (MAIAC)

393   satellite-derived Aerosol Optical Depth (AOD) that Canadian and western US fires have

394   caused an increase in the daily $PM_{2.5}$ over Montana, North Dakota, South Dakota and

395   Minnesota by 18.3, 12.8, 10.4 and 10.1 $\mu g\ m^{-3}$, respectively, between August 2011 (a low

396   fire month) and August 2018 (a high fire month). In summary, the visually apparent satellite-

397   based signatures of wildfire-smoke across Canada and EUS provide a necessary, though not

398   sufficient, support for the influence of Canadian smoke plumes on EUS air quality. Although,

399   the change in burnt area over northeastern EUS is negligible compared to the western US and

400   Canadian regions, however, there are some enhancements seen over east coast of US, which

401   can also contribute to enhanced fire emissions.

402
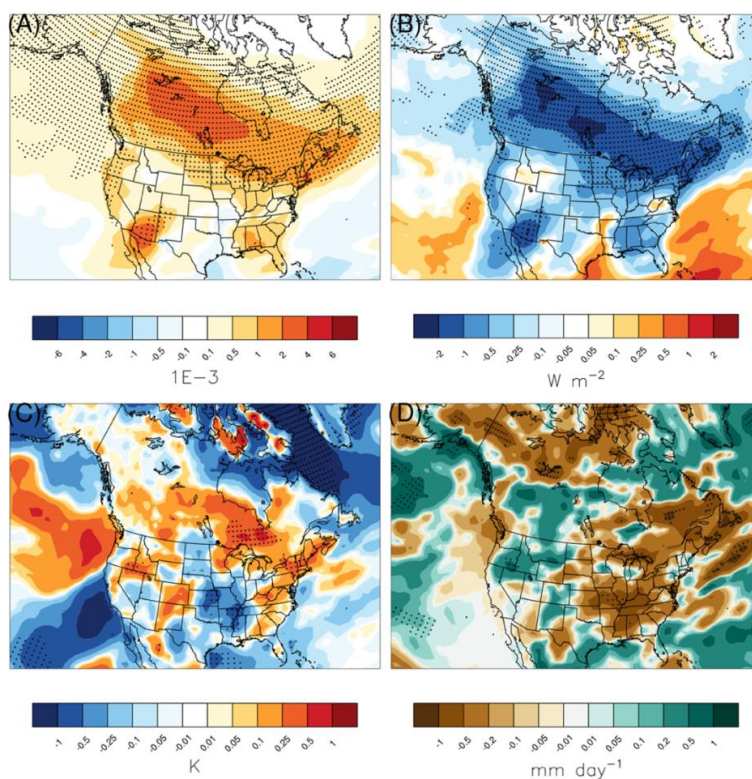
Figure 5: Spatial distribution of decadal mean summer (JJA) wildfire-induced future changes
[(2050ALL-2050WEF) – (2000ALL-2000WEF)]. A) aerosol absorption optical depth at 550 nm, B)
aerosol direct radiative forcing at surface, C) lower-tropospheric stability calculated as the
difference between the potential temperature at 900 hPa and 1000 hPa, D) summer averaged
precipitation rates, over North America. Areas marked with black dots indicate grids where
changes are significant at the 95% confidence level.

409   Secondly, distinct climatic feedbacks are also simulated which contributes to

410   enhancement of EUS pollution. Specifically, the enhancement of wildfire-induced smoke

411   aerosols increases solar absorption and scattering in the future (Figure 5A). This reduces the

412   incoming solar radiation at the surface (Figure 5B) and induces surface cooling. With

413   atmospheric warming and surface cooling, lower-tropospheric stability is enhanced by

414   wildfire aerosols in the future (Figure 5C). These changes impose a thermal capping that

415   traps more anthropogenic aerosols and particulate matter near the surface over EUS. At the

416   same time, future increase in wildfire emissions also leads to greater reduction of monthly

417   rainfall (Figure 5D) over EUS, which may subsequently strengthen the positive feedback to

418   surface $PM_{2.5}$ over EUS by reducing wet scavenging of transported wildfire smoke to EUS.

419   Thus, wildfire-emitted aerosols induce positive feedback on the surface $PM_{2.5}$ concentration

420   over EUS through fire-climate interactions that vary on a regional scale. However, due to

421   computational constrains, no direct quantification of the magnitude of these feedback (with

422   aerosol-radiation and aerosol-cloud interactions turned off) on PM2.5 is performed and would

423   be taken up in future studies.

424   Lastly, the reason of why the contribution of wildfire emissions to the total surface

425    $PM_{2.5}$ in EUS is so substantial in the 2050s is the drastic reduction of anthropogenic

426   contribution to the surface $PM_{2.5}$ over EUS in the future primarily due to policy-driven

427   reduction in anthropogenic emissions under the RCP4.5 scenario. Specifically, the simulated

428   ambient summer mean $PM_{2.5}$ concentration exhibits widespread declines in the future

429   (Supplementary Figure 3), with reduction in $PM_{2.5}$ concentration over eastern US in the range

430   of 4-15 $\mu g/m^3$, which is greatest within North America. Thus, large reduction in

431   anthropogenic contribution combined with increased downwind advection of Canadian

432   smoke to EUS and the associated positive feedbacks can explain the projected dominance of

433   wildfire emissions over EUS in future.

434   **3.4 Future Implications and uncertainties**

435   However, is the simulated future enhancement in wildfire contribution over EUS

436   substantial enough to affect the surface $PM_{2.5}$ values over EUS in future? The World Health

437   Organization (WHO) air quality guidelines for annual and daily $PM_{2.5}$ concentration are 10

438    $\mu g\ m^{-3}$ and 25 $\mu g\ m^{-3}$, respectively. As no specific guideline for seasonal-mean $PM_{2.5}$ in the

439   summer is available, we use the annual guideline value as a reference to understand the

440   implication of wildfire emissions on ambient $PM_{2.5}$ concentration in the future. Interestingly,

the mean summertime PM$_{2.5}$ concentration in the wildfire emission free (WEF) scenario is projected to remain within 10 µg m^{-3} over most of North America, except for the southeastern US (Figure 6A). However, the ALL-scenario projects an increase in the exposure concentration level such that values > 10 µg/m^3 are common in Canada and EUS in the future (Figure 6B). Quantitatively, over Canada, the entire PDF of PM$_{2.5}$ concentration shifts towards higher values by ~5-6 µg/m^3. Specifically, the modal value shifts from ~ 6 µg/m^3 in 2050$_{WEF}$ to 11-12 µg/m^3 in 2050$_{ALL}$ (Figure 6C), so PM$_{2.5}$ concentration is projected to surpass the WHO guidelines over a large fraction of Canada in the future. Similarly, the entire PDF of PM$_{2.5}$ concentration shifts towards higher values by ~2-3 µg/m^3 over EUS, with the mode of the PDF increasing from ~ 7-8 µg/m^3 in 2050$_{WEF}$ to ~ 10-11 µg/m^3 in 2050$_{ALL}$ (Figure 6E). The modal value of summer mean PM$_{2.5}$ over WUS increases from ~ 6 µg/m^3 in 2050$_{WEF}$ to ~ 7-8 µg/m^3 in 2050$_{ALL}$ (Figure 6D), although a few grid cells show PM$_{2.5}$ values greater than 10 µg/m^3 (Figure 6B).

Clearly, the climate-induced enhancement in fires and its influence via the advected wildfire smoke to EUS can have significant implications for air quality management in the future. The PM2.5 enhancement in future over the southern states within EUS is large (Figure 6A-B), which is consistent with Figure 3 and 4 results. However, the future change in burnt area over the same region is negligible or mostly reducing (Figure 1C-D). Thus, it can be argued that the simulated enhancement is mostly related with the positive climatic feedbacks due to wildfire emissions i.e. enhanced lower atmospheric stability and reduced surface precipitation (Figure 5). As the rate of anthropogenic emissions is also regionally highest over the Southeastern states, the impact of these wildfire-induced climatic feedbacks on local air quality is distinctly seen over the EUS.

464
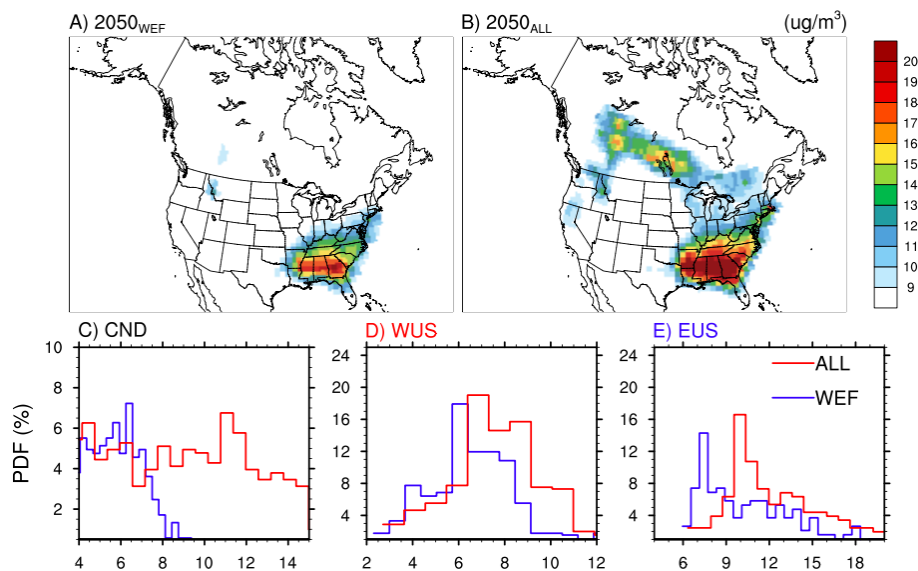
Figure 6: **Spatial distribution and probability density function of** PM$_{2.5}$ **concentration in 2050s. A-B,** Spatial distribution of decadal-average summer (JJA) mean PM$_{2.5}$ concentration over North America in mid-21st century from 2050$_{WEF}$ (wildfire emission-free) (A) and 2050$_{ALL}$ (wildfire emission-inclusive) (B). **C-E,** Probability density functions (PDFs) of the same within the three regions shown in Figure 2B for Canada; CND (C), western US; WUS (D), and eastern US; EUS (E), respectively, for the 2050$_{WEF}$ (blue) and 2050$_{ALL}$ (red) runs. The y-axis indicates the probability of occurrence of different PM$_{2.5}$ values shown in the x-axis. Only grids over land in North America are used to generate the PDFs. Note the different ranges of values shown in the y- and x-axis in **C-E.** The colorbar and the x-axis for Panel C-E indicates PM$_{2.5}$ values.

Note that our simulated present-day estimates of wildfire induced PM$_{2.5}$ values as well as the percentage contribution of wildfire emissions are within the range of reported values in previous studies over the domain, which augment the fidelity our future projections. Specifically, our simulated present-day estimates of wildfire induced PM$_{2.5}$ values are also within the range of reported values in previous studies over the domain. Reported values of wildfire-induced PM$_{2.5}$ over WUS during summertime vary from ~1 µg/m^3 (Jaffe et al., 2008) to ~2 µg/m^3 (Park et al., 2007) and ~3 µg/m^3 (Ford et al., 2018), with the highest values documented over the Pacific Northwest and west coast regions (~1-4 µg/m^3) (O'Dell et al., 2019). The wildfire-induced PM$_{2.5}$ over EUS during summertime varies from ~1 µg/m^3 (Park

484   et al., 2007) to ~2.5 µg/m^3 (~ 3 µg/m^3 in the southeastern US) (Ford et al., 2018).

485   Consistently, our simulated present-day estimates of wildfire contribution values are also

486   within the range of reported values in previous studies. For example, Meng et al. (2019)

487   found that wildfires can be the largest sectoral contributor (~18-59%) to the population-

488   weighted PM$_{2.5}$ in various subregions of Canada. Over WUS, the present-day percentage

489   contribution of wildfire induced PM$_{2.5}$ to the total PM$_{2.5}$ is reported to be ~ 12% (Liu et al.,

490   2017), ~ 15% (Park et al., 2007) and ~30% (Ford et al., 2018), with higher values of ~40% in

491   the Pacific Northwest (O'Dell et al., 2019). Over EUS our simulated values are also within

492   the range of previously reported values of ~ 5% (Park et al., 2007) and ~15-18% (Ford et al.,

493   2018). However, our two-way coupled simulations illustrate that future enhancement in the

494   wildfire associated PM$_{2.5}$ over the EUS could be greater compared to the western US, which

495   is not emphasized explicitly in any of the previous studies (although Ford et al., 2018

496   illustrated increase in PM2.5 over mid and central US from Canadian fires). These could be

497   since inclusion of the wildfire-induced climatic feedbacks in our simulation is an

498   unprecedented exercise. Please also note that our study is focused on JJA period and the

499   wildfires in western US mainly occurs during August-September months, so the results

500   should be compared consciously.

501   Nonetheless, inherent limitations in our simulations may introduce uncertainties in the

502   projected future changes. For example, our reported changes in PM$_{2.5}$ concentrations based on

503   relatively coarse resolution simulations and decadal averages likely represent a low-end

504   estimate compared to changes at regional and daily/weekly scales. Moreover, our

505   experiments do not consider the direct human influences such as population change and

506   socioeconomic development on wildfires, which may aggravate the increase in PM$_{2.5}$

507   concentrations over the densely populated EUS in the future. Common sources of uncertainty

508   in modeling burnt area and fire emission and fire aerosol and smoke are also present in our

509   model. Fire smoke, in particular, is extremely hard to measure and evaluate. Lastly, inherent

510   uncertainties in the physics parameterizations used in the model, sensitivity of climate to

511   GHGs emissions, and the RCP scenarios should also be noted. Thus, ensemble modeling

512   considering different emissions scenarios, population and future time periods, and the use of

513   a finer spatial resolution may provide a more robust and better quantification of the wildfire-

514   induced impact on policy regulated improvements in $PM_{2.5}$ over EUS.

515   **4. Conclusion**

516   In summary, online coupled fire-climate-ecosystem simulations project a nearly

517   twofold increase in wildfire-induced summer-mean surface $PM_{2.5}$ concentration by the mid-

518   21st century over the entire North America. In a wildfire-emission free future, a large portion

519   of North America will have $PM_{2.5}$ values below the WHO guidelines. But in a future with

520   wildfire emissions, the improvements from policy-driven reductions in anthropogenic $PM_{2.5}$

521   will be compromised by the projected doubling of $PM_{2.5}$ from wildfires. More strikingly,

522   wildfire-induced enhancement in surface $PM_{2.5}$ values and percentage contribution of the

523   wildfire emissions over EUS could be substantial by mid-century. This is mainly because of

524   the large enhancement in fires over Northern America by 2050s and associated increase in

525   amount of downwind transport of smoke to EUS. In addition, enhancement of smoke

526   transport induces a positive climate feedback to $PM_{2.5}$ concentrations over EUS by increasing

527   the lower-tropospheric stability and reducing wet scavenging rates. Despite the inherent

528   limitations, this study highlights the natural versus anthropogenic contributions and the non-

529   local nature of air pollution that can complicate regulatory strategies aimed at improving air

530   quality over the eastern US in a warmer future.

531   **Data availability statements**

532 The HMS data used in this paper are available free through the link
533 https://www.ospo.noaa.gov/Products/land/hms.html. The model simulations data are
534 available at https://portal.nersc.gov/project/m1660/yang560/wildfire

535 **Code availability statements**

536 The model code and scripts are available at
537 https://portal.nersc.gov/project/m1660/yang560/wildfire

538

539 **Acknowledgements:**

540 This research was performed at PNNL and funded under Assistance Agreement No.
541 RD835871 by the U.S. Environmental Protection Agency to Yale University through the
542 SEARCH (Solutions for Energy, AiR, Climate, and Health) Center. It has not been formally
543 reviewed by EPA. The views expressed in this document are solely those of the SEARCH
544 Center and do not necessarily reflect those of the Agency. EPA does not endorse any
545 products or commercial services mentioned in this publication. CS is supported by the New
546 Faculty Initiation Grant project number CE/20-21/065/NFIG/008961 from IIT Madras.
547 PNNL is operated by Battelle Memorial Institute for the U.S. Department of Energy under
548 contract DE-AC06-76RLO-1830.
549

550 **Authors Contribution**

551 YQ, CS and RL designed this study. CS did the model and satellite analysis and wrote the
552 first draft of the manuscript. YZou performed the simulations. All authors provided inputs
553 throughout the study and helped in the drafting and submission process.
554

555 **References**

556 Abatzoglou, J. T. and Williams, A. P.: Impact of anthropogenic climate change on wildfire
557 across western US forests, Proc. Natl. Acad. Sci., 113(42), 11770 LP – 11775,
558 doi:10.1073/pnas.1607171113, 2016.

559 Andela, N., Morton, D. C., Giglio, L., Chen, Y., van der Werf, G. R., Kasibhatla, P. S.,
560 DeFries, R. S., Collatz, G. J., Hantson, S., Kloster, S., Bachelet, D., Forrest, M., Lasslop, G.,
561 Li, F., Mangeon, S., Melton, J. R., Yue, C. and Randerson, J. T.: A human-driven decline in
562 global burned area, Science (80-.)., 356(6345), 1356 LP – 1362,
563 doi:10.1126/science.aal4108, 2017.

564 Anjali, H., Muhammad, A., Anthony, D. M., Karen, S., R., S. M., Mick, M., M., T. A., J., A.
565 M. and Martine, D.: Impact of Fine Particulate Matter (PM$_{2.5}$) Exposure During Wildfires on
566 Cardiovascular Health Outcomes, J. Am. Heart Assoc., 4(7), e001653,
567 doi:10.1161/JAHA.114.001653, 2019.

568 Black, C., Tesfaigzi, Y., Bassein, J. A. and Miller, L. A.: Wildfire smoke exposure and
569 human health: Significant gaps in research for a growing public health issue, Environ.
570 Toxicol. Pharmacol., 55, 186–195, doi:https://doi.org/10.1016/j.etap.2017.08.022, 2017.

571 Brey, S. J., Ruminski, M., Atwood, S. A. and Fischer, E. V: Connecting smoke plumes to

sources using Hazard Mapping System (HMS) smoke and fire location data over North America, Atmos. Chem. Phys., 18(3), 1745–1761, doi:10.5194/acp-18-1745-2018, 2018.

Dempsey, F.: Forest Fire Effects on Air Quality in Ontario: Evaluation of Several Recent Examples, Bull. Am. Meteorol. Soc., 94(7), 1059–1064, doi:10.1175/BAMS-D-11-00202.1, 2013.

Dominici, F., Peng, R. D., Bell, M. L., Pham, L., McDermott, A., Zeger, S. L. and Samet, J. M.: Fine Particulate Air Pollution and Hospital Admission for Cardiovascular and Respiratory Diseases, JAMA, 295(10), 1127–1134, doi:10.1001/jama.295.10.1127, 2006.

Diao, M., Holloway, T., Choi, S., O'Neill, S.M., Al-Hamdan, M.Z., Van Donkelaar, A., Martin, R.V., Jin, X., Fiore, A.M., Henze, D.K. and Lacey, F., 2019. Methods, availability, and applications of PM2. 5 exposure estimates derived from ground measurements, satellite, and atmospheric models. *Journal of the Air & Waste Management Association*, *69*(12), pp.1391-1414.

Ford, B., Val Martin, M., Zelasky, S. E., Fischer, E. V, Anenberg, S. C., Heald, C. L. and Pierce, J. R.: Future Fire Impacts on Smoke Concentrations, Visibility, and Health in the Contiguous United States, GeoHealth, 2(8), 229–247, doi:10.1029/2018GH000144, 2018.

Gillett, N. P., Weaver, A. J., Zwiers, F. W. and Flannigan, M. D.: Detecting the effect of climate change on Canadian forest fires, Geophys. Res. Lett., 31(18), doi:10.1029/2004GL020876, 2004.

Gunsch, M. J., May, N. W., Wen, M., Bottenus, C. L. H., Gardner, D. J., VanReken, T. M., Bertman, S. B., Hopke, P. K., Ault, A. P. and Pratt, K. A.: Ubiquitous influence of wildfire emissions and secondary organic aerosol on summertime atmospheric aerosol in the forested Great Lakes region, Atmos. Chem. Phys., 18(5), 3701–3715, doi:10.5194/acp-18-3701-2018, 2018.

Guan S, Wong DC, Gao Y, Zhang T, Pouliot G. Impact of wildfire on particulate matter in the southeastern United States in November 2016. Sci Total Environ. 2020;724:138354. doi:10.1016/j.scitotenv.2020.138354.

Johnston F. H., Henderson. S. B., Yang, C., T., R. J., Miriam, M., S., D. R., Patrick, K., M.J.S., B. D. and Michael, B.: Estimated Global Mortality Attributable to Smoke from Landscape Fires, Environ. Health Perspect., 120(5), 695–701, doi:10.1289/ehp.1104422, 2012.

Harris, R. M. B., Remenyi, T. A., Williamson, G. J., Bindoff, N. L., and Bowman, D. M. J. S.: Climate-vegetation fire interactions and feedbacks: trivial detail or major barrier to projecting the future of the Earth system?, Wires Clim. Change, 7, 910-931, 10.1002/wcc.428, 2016.

Hantson, S., Arneth, A., Harrison, S. P., Kelley, D. I., Prentice, I. C., Rabin, S. S., et al. (2016). The status and challenge of global fire modelling. Biogeosciences, 13, 3359–3375. https://doi.org/10.5194/bg-13-3359-2016

Hu, X., Yu, C., Tian, D., Ruminski, M., Robertson, K., Waller, L. A. and Liu, Y.: Comparison of the Hazard Mapping System (HMS) fire product to ground-based fire records in Georgia, USA, J. Geophys. Res. Atmos., 121(6), 2901–2910, doi:10.1002/2015JD024448, 2016.

614 HURTT, G. C., FROLKING, S., FEARON, M. G., MOORE, B., SHEVLIAKOVA, E.,
615 MALYSHEV, S., PACALA, S. W. and HOUGHTON, R. A.: The underpinnings of land-use
616 history: three centuries of global gridded land-use transitions, wood-harvest activity, and
617 resulting secondary lands, Glob. Chang. Biol., 12(7), 1208–1229, doi:10.1111/j.1365-
618 2486.2006.01150.x, 2006.

619 Jaffe, D., Hafner, W., Chand, D., Westerling, A. and Spracklen, D.: Interannual Variations in
620 $PM_{2.5}$ due to Wildfires in the Western United States, Environ. Sci. Technol., 42(8), 2812–
621 2818, doi:10.1021/es702755v, 2008.

622 Jolly, W. M., Cochrane, M. A., Freeborn, P. H., Holden, Z. A., Brown, T. J., Williamson, G.
623 J. and Bowman, D. M. J. S.: Climate-induced variations in global wildfire danger from 1979
624 to 2013, Nat. Commun., 6, 7537 [online] Available from:
625 https://doi.org/10.1038/ncomms8537, 2015.

626 Kaulfus, A. S., Nair, U., Jaffe, D., Christopher, S. A. and Goodrick, S.: Biomass Burning
627 Smoke Climatology of the United States: Implications for Particulate Matter Air Quality,
628 Environ. Sci. Technol., 51(20), 11731–11741, doi:10.1021/acs.est.7b03292, 2017.

629 Kirchmeier-Young, M. C., Zwiers, F. W., Gillett, N. P. and Cannon, A. J.: Attributing
630 extreme fire risk in Western Canada to human emissions, Clim. Change, 144(2), 365–379,
631 doi:10.1007/s10584-017-2030-0, 2017.

632 Kitzberger, T., Falk, D. A., Westerling, A. L. and Swetnam, T. W.: Direct and indirect
633 climate controls predict heterogeneous early-mid 21st century wildfire burned area across
634 western and North America, PLoS One, 12(12), e0188486 [online] Available from:
635 https://doi.org/10.1371/journal.pone.0188486, 2017.

636 Knorr, W., Dentener, F., Lamarque, J.-F., Jiang, L. and Arneth, A.: Wildfire air pollution
637 hazard during the 21st century, Atmos. Chem. Phys., 17(14), 9223–9236, doi:10.5194/acp-
638 17-9223-2017, 2017.

639 Koplitz, S.N., Nolte, C.G., Pouliot, G.A., Vukovich, J.M. and Beidler, J., 2018. Influence of
640 uncertainties in burned area estimates on modeled wildland fire PM2. 5 and ozone pollution
641 in the contiguous US. *Atmospheric environment*, *191*, pp.328-339.

642 Lamarque, J. F., Bond, T. C., Eyring, V., Granier, C., Heil, A., Klimont, Z., Lee, D., Liousse,
643 C., Mieville, A., Owen, 628 B., Schultz, M. G., Shindell, D., Smith, S. J., Stehfest, E., Van
644 Aardenne, J., Cooper, O. R., Kainuma, M., 629 Mahowald, N., McConnell, J. R., Naik, V.,
645 Riahi, K., and van Vuuren, D. P.: Historical (1850-2000) gridded anthropogenic and biomass
646 burning emissions of reactive gases and aerosols: methodology and application, 631 Atmos.
647 Chem. Phys., 10, 7017-7039, 10.5194/acp-10-7017-2010, 2010.

648 Leibensperger, E. M., Mickley, L. J., Jacob, D. J., Chen, W.-T., Seinfeld, J. H., Nenes, A.,
649 Adams, P. J., Streets, D. G., Kumar, N. and Rind, D.: Climatic effects of 1950–2050
650 changes in US anthropogenic aerosols – Part 2: Climate response, Atmos. Chem.
651 Phys., 12(7), 3349–3362, doi:10.5194/acp-12-3349-2012, 2012.

652 Li, F., Zeng, X. D., & Levis, S. (2012). A process-based fire parameterization of intermediate
653 complexity in a dynamic global vegetation model. Biogeosciences, 9(7), 2761–2780.
654 https://doi.org/10.5194/bg-9-2761-2012

655 Liu, J. C., Mickley, L. J., Sulprizio, M. P., Dominici, F., Yue, X., Ebisu, K., Anderson, G. B.,
656 Khan, R. F. A., Bravo, M. A. and Bell, M. L.: Particulate Air Pollution from Wildfires in the

657   Western US under Climate Change, Clim. Change, 138(3), 655–666, doi:10.1007/s10584-
658   016-1762-6, 2016.

659   Liu, Y., Goodrick, S. and Heilman, W.: Wildland fire emissions, carbon, and climate:
660   Wildfire–climate interactions, For. Ecol. Manage., 317, 80–96,
661   doi:https://doi.org/10.1016/j.foreco.2013.02.020, 2014.

662   Liu, X., Easter, R. C., Ghan, S. J., Zaveri, R., Rasch, P., Shi, X., Lamarque, J. F., Gettelman,
663   A., Morrison, H., Vitt, F., Conley, A., Park, S., Neale, R., Hannay, C., Ekman, A. M. L.,
664   Hess, P., Mahowald, N., Collins, W., Iacono, M. J., Bretherton, C. S., Flanner, M. G., and
665   Mitchell, D.: Toward a minimal representation of aerosols in climate models: description and
666   evaluation in the Community Atmosphere Model CAM5, Geosci. Model Dev., 5, 709- 652
667   739, 10.5194/gmd-5-709-2012, 2012.

668   Meng, J., Martin, R.V., Li, C., van Donkelaar, A., Tzompa-Sosa, Z.A., Yue, X., Xu, J.W.,
669   Weagle, C.L. and Burnett, R.T., 2019. Source Contributions to Ambient Fine Particulate
670   Matter for Canada. *Environmental science & technology*, *53*(17), pp.10269-10278.

671   McClure, C. D. and Jaffe, D. A.: US particulate matter air quality improves except in
672   wildfire-prone areas, Proc. Natl. Acad. Sci., 115(31), 7901 LP – 7906,
673   doi:10.1073/pnas.1804353115, 2018.

674   Neale, R. B., Chen, C. C., Gettelman, A., Lauritzen, P. H., Park, S., Williamson, D. L.,
675   Conley, A. J., Garcia, R., Kinnison, D., Lamarque, J. F., Marsh, D., Mills, M., Smith, A. K.,
676   Tilmes, S., Vitt, F., Morrison, H., Cameron671 Smith, P., Collins, W. D., Iacono, M. J.,
677   Easter, R. C., Ghan, S. J., Liu, X. H., Rasch, P. J., and Taylor, M. A.: Description of the
678   NCAR Community Atmosphere Model (CAM 5.0), NCAR 289, 2013

679   Nolte, C. G., Spero, T. L., Bowden, J. H., Mallard, M. S. and Dolwick, P. D.: The potential
680   effects of climate change on air quality across the conterminous US at 2030 under three
681   Representative Concentration Pathways, Atmos. Chem. Phys., 18(20), 15471–15489,
682   doi:10.5194/acp-18-15471-2018, 2018.

683   Katelyn O'Dell, Bonne Ford, Emily V. Fischer, and Jeffrey R. Pierce Environmental Science
684   & Technology 2019 53 (4), 1797-1804, DOI: 10.1021/acs.est.8b05430.

685
686   Partain, J. L., Alden, S., Strader, H., Bhatt, U. S., Bieniek, P. A., Brettschneider, B. R.,
687   Walsh, J. E., Lader, R. T., Olsson, P. Q., Rupp, T. S., Thoman, R. L., York, A. D. and Ziel,
688   R. H.: An Assessment of the Role of Anthropogenic Climate Change in the Alaska Fire
689   Season of 2015, Bull. Am. Meteorol. Soc., 97(12), S14–S18, doi:10.1175/BAMS-D-16-
690   0149.1, 2016.

691   Park, S., Bretherton, C. S., and Rasch, P. J.: Integrating Cloud Processes in the Community
692   Atmosphere Model, Version 5, J. Climate, 27, 6821-6856, 10.1175/Jcli-D-14-00087.1, 2014.

693   Park, R.J., Jacob, D.J. and Logan, J.A., 2007. Fire and biofuel contributions to annual mean
694   aerosol mass concentrations in the United States. *Atmospheric Environment*, *41*(35), pp.7389-
695   7400.

696   Pierce, J. R., Val Martin, M., & Heald, C. L. (2017). Estimating the Effects of Changing
697   Climate on Fires and Consequences for U.S. Air Quality, Using a Set of Global and Regional
698   Climate Models (final report no. JFSP-13-1-01-4). Retrieved from
699   https://www.firescience.gov/projects/ 13-1-01-4/project/13-1-01-4_final_report.pdf

700   Pouliot G, Pace TG, Roy B, Pierce T, Mobley D. Development of a biomass burning
701   emissions inventory by combining satellite and ground-based information. J Appl Remote
702   Sens. 2008;2:021501. doi: 10.1117/1.2939551.

703   Randerson, J. T., Chen, Y., van der Werf, G. R., Rogers, B. M., & Morton, D. C. (2012).
704   Global burned area and biomass burning emissions from small fires. Journal of Geophysical
705   Research, 117, G04012. https://doi.org/10.1029/2012JG002128

706   Rolph, G. D., Draxler, R. R., Stein, A. F., Taylor, A., Ruminski, M. G., Kondragunta, S.,
707   Zeng, J., Huang, H.-C., Manikin, G., McQueen, J. T. and Davidson, P. M.: Description and
708   Verification of the NOAA Smoke Forecasting System: The 2007 Fire Season, Weather
709   Forecast., 24(2), 361–378, doi:10.1175/2008WAF2222165.1, 2009.

710   Spracklen, D. V., Mickley, L. J., Logan, J. A., Hudman, R. C., Yevich, R., Flannigan, M. D.,
711   & Westerling, A. L. (2009). Impacts of climate change from 2000 to 2050 on wildfire activity
712   and carbonaceous aerosol concentrations in the western United States. Journal of Geophysical
713   Research, 114, D20301. https://doi.org/10.1029/2008JD010966

714   Sun, Y., Gu, L. H., and Dickinson, R. E.: A numerical issue in calculating the coupled carbon
715   and water fluxes in a climate model, J. Geophys. Res.-Atmos., 117,
716   D2210310.1029/2012jd018059, 2012

717   Sofiev, M., Ermakova, T., and Vankevich, R.: Evaluation of the smoke-injection height from
718   wild-land fires using remote-sensing data, Atmos. Chem. Phys., 12, 1995-2006, 10.5194/acp-
719   12-1995-2012, 2012

720   Shi, H., Jiang, Z., Zhao, B., Li, Z., Chen, Y., Gu, Y., Jiang, J. H., Lee, M., Liou, K.-N., Neu,
721   J. L., Payne, V. H., Su, H., Wang, Y., Witek, M. and Worden, J.: Modeling Study of the Air
722   Quality Impact of Record-Breaking Southern California Wildfires in December 2017, J.
723   Geophys. Res. Atmos., 0(0), doi:10.1029/2019JD030472, 2019.

724   U.S. EPA (U.S. Environmental Protection Agency). 2009. Integrated Science Assessment
725   (ISA) For Particulate Matter (Final Report). EPA/600/R-08/139F.Washington, DC:U.S. EPA.

726   U.S. EPA. 2018. Our Nation's Air. https://gispub.epa.gov/air/trendsreport/2018/

727   Val Martin, M., Heald, C. L., Lamarque, J.-F., Tilmes, S., Emmons, L. K. and Schichtel, B.
728   A.: How emissions, climate, and land use change will impact mid-century air quality over the
729   United States: a focus on effects at national parks, Atmos. Chem. Phys., 15(5), 2805–2823,
730   doi:10.5194/acp-15-2805-2015, 2015.

731   Van der Werf, G. R., Randerson, J. T., Giglio, L., Collatz, G. J., Kasibhatla, P. S., and
732   Arellano, A. F.: Interannual variability in global biomass burning emissions from 1997 to
733   2004, Atmos. Chem. Phys., 6, 3423-3441, DOI 737 10.5194/acp-6-3423-2006, 2006

734   Van Der Werf, G. R., Randerson, J. T., Giglio, L., Collatz, G. J., Mu, M., Kasibhatla, P. S.,
735   Morton, D. C., Defries, R. S., Jin, Y. and Van Leeuwen, T. T.: Global fire emissions and the
736   contribution of deforestation, savanna, forest, agricultural, and peat fires (1997-2009), Atmos.
737   Chem. Phys., 10(23), 11707–11735, doi:10.5194/acp-10-11707-2010, 2010.

738   Van Donkelaar, A., R. V. Martin, M. Brauer, N. C. Hsu, R. A. Kahn, R. C. Levy, A.
739   Lyapustin, A. M. Sayer, and D. M. Winker. 2018. Global Annual PM$_{2.5}$ Grids from MODIS,
740   MISR and SeaWiFS Aerosol Optical Depth (AOD) with GWR, 1998-2016. Palisades NY:

741   NASA Socioeconomic Data and Applications Center (SEDAC).
742   https://doi.org/10.7927/H4ZK5DQS. Accessed 16 November 2019.

743   Ward, D. S., Kloster, S., Mahowald, N. M., Rogers, B. M., Randerson, J. T. and Hess, P. G.:
744   The changing radiative forcing of fires: global model estimates for past, present and future,
745   Atmos. Chem. Phys., 12(22), 10857–10886, doi:10.5194/acp-12-10857-2012, 2012.

746   Wotton, B. M., Flannigan, M. D., and Marshall, G. A.: Potential climate change impacts on
747   fire intensity and key wildfire suppression thresholds in Canada, Environ. Res. Lett., 12,
748   095003, https://doi.org/10.1088/1748-9326/aa7e6e, 2017.

749   Westerling, A. L., Hidalgo, H. G., Cayan, D. R. and Swetnam, T. W.: Warming and Earlier
750   Spring Increase Western U.S. Forest Wildfire Activity, Science (80-.)., 313(5789), 940 LP –
751   943, doi:10.1126/science.1128834, 2006.

752   Wotawa, G. and Trainer, M.: The Influence of Canadian Forest Fires on Pollutant
753   Concentrations in the United States, Science (80-.)., 288(5464), 324 LP – 328,
754   doi:10.1126/science.288.5464.324, 2000.

755   Wu, Y., Arapi, A., Huang, J., Gross, B. and Moshary, F.: Intra-continental wildfire smoke
756   transport and impact on local air quality observed by ground-based and satellite remote
757   sensing in New York City, Atmos. Environ., 187, 266–281,
758   doi:https://doi.org/10.1016/j.atmosenv.2018.06.006, 2018.

759   Xue, Z., Gupta, P., and Christopher, S.: Satellite-based estimation of the impacts of
760   summertime wildfires on PM2.5concentration in the United States, Atmos. Chem. Phys., 21,
761   11243–11256, https://doi.org/10.5194/acp-21-11243-2021, 2021.

762   Yang, P.-L., Y. Zhang, K. Wang, P. Doraiswamy, and S.-H. Cho, 2019, Health Impacts and
763   Cost-Benefit Analyses of Surface O$_3$ and PM$_{2.5}$ over the U.S. under Future Climate and
764   Emission Scenarios, _Environmental Research_, 178, November 2019, 108687,
765   https://doi.org/10.1016/j.envres.2019.108687.

766   Yue, X., Mickley, L. J., Logan, J. A. and Kaplan, J. O.: Ensemble projections of wildfire
767   activity and carbonaceous aerosol concentrations over the western United States in the mid-
768   21st century, Atmos. Environ., 77, 767–780,
769   doi:https://doi.org/10.1016/j.atmosenv.2013.06.003, 2013.

770   Zou, Y., Wang, Y., Ke, Z., Tian, H., Yang, J. and Liu, Y.: Development of a REgion-Specific
771   Ecosystem Feedback Fire (RESFire) Model in the Community Earth System Model, J. Adv.
772   Model. Earth Syst., 11(2), 417–445, doi:10.1029/2018MS001368, 2019.

773   Zou, Y., Wang, Y., Qian, Y., Tian, H., Yang, J. and Alvarado, E.: Using CESM-RESFire to
774   understand climate–fire–ecosystem interactions and the implications for decadal climate
775   variability, Atmos. Chem. Phys., 20, 995–1020, https://doi.org/10.5194/acp-20-995-2020,
776   2020.

777   Zhang, Y., P.-L. Yang, Y. Gao, R. L. Leung, and M. Bell, 2020, Health and Economic
778   Impacts of Air Pollution Induced by Climate Extremes over the Continental U.S.,
779   _Environmental International_, 143, 105921, https://doi.org/10.1016/j.envint.2020.105921.

780

781